

Electrochemical Sensor Based on Silver Nanoparticles/Multi-walled Carbon Nanotubes Modified Glassy Carbon Electrode to Detect Cyanide in Food Products

Hongyuan Zhang^{1,*}, Dawei Sun², Tieping Cao¹

¹ Department of Chemistry, Baicheng Normal University, Baicheng 137000, China

² Department of Chemistry, Jilin Normal University, Changchun 130000, China

*E-mail: october_hy_zhang@163.com

Received: 5 December 2019 / Accepted: 31 January 2020 / Published: 10 March 2020

In this study, silver nanoparticles/carbon nanotubes (Ag NPs/CNTs) was successfully synthesized on the surface of glassy carbon (GC) electrode using a facile chemical technique to evaluate determination of cyanide as a toxic substance in food products. The structural properties of synthesized CNTs and Ag NPs/CNTs were studied by scanning electron microscope, energy dispersive X-Ray and X-Ray diffraction analyses. The voltammetric and amperometric techniques were used for electrochemical studies of modified electrodes. The structural studies showed high density, porosity and aspect ratio of the Ag NPs/CNTs electrodes. The cycle voltammetric studies of Ag NPs/CNTs/GC electrode showed sharp and stable oxidation peak at 0.75 V in pH 7 for cyanide. Amperometry results exhibited that Ag NPs/CNTs/GC electrode was sensitive, selective and stable to determinate cyanide. The linear range, sensitivity, and detection limit of modified sensor were 0.1 to 210 μM , 0.7192 $\mu\text{A}/\mu\text{M}$ and 4 nM, respectively which were better values than those obtained in previous researches. Study on the interfere effect of Br^- , SO_3^{2-} , CH_3COO^- , I^- , $\text{C}_2\text{O}_4^{2-}$, Cl^- , SO_4^{2-} , CO_3^{2-} , Ni^{+2} , Co^{2+} , HPO_4^{-2} , F^- and Zn^{+2} analytes showed that there was not any interfere in determination of cyanide on Ag NPs/CNTs/GC electrode surface. The recorded amperometric results of real sample showed the modified electrode was successfully applied for cyanide detection in apricot juice.

Keywords: Carbon nanotubes; Ag nanoparticles; Cyanide; Electrochemical sensor; Apricot juice

1. INTRODUCTION

The monitoring of water and food quality is important activity of Food and Drug Administration (FDA) and many of related health organizations in the world [1]. Phosphates, sulfates, nitrates and cyanides are the most common contaminations in agriculture and drinking waters due to chemical fertilizers and industrial processes [2]. Among them, Cyanides are rapidly acting and highly toxic components that can be created in various forms such as colorless gas (hydrogen cyanide and cyanogen

chloride) and crystal form (sodium cyanide and potassium cyanide) [3, 4]. Moreover, these components can be produced in agricultural species such as cassava, flax, sorghum, alfalfa, bamboo, peach, pear, cherry, plum, corn, potato, cotton, almond, and beans [5].

Cyanides are various application such as paper, textiles, photographs, metallurgy, pesticides and plastics industries [6]. By considering the highly toxic nature of cyanides, these components can be contaminated the environment and lead to poisoning [7, 8]. The poisoning may result in seizures, slow heart rate, low blood pressure, loss of consciousness, and cardiac arrest. Therefore, it is increasingly important to study and monitor cyanides in the environment.

Thus, it is necessary to study and develop the sensing tools and techniques to determine cyanide in real samples. Various techniques are used for detection of cyanide, such as spectrophotometry, capillary electrophoresis, fluorometry, chemiluminescence, near-infrared cavity ring down spectroscopy, atomic absorption spectrometry, mass spectrometry, gas chromatography, quartz crystal mass monitors and electrochemical methods[9-11]. Most of these techniques are sensitive and precise but they are expensive and time-consuming. Among these techniques, electrochemical methods such as cyclic voltammetry and amperometry are fast response and low-cost techniques in determining cyanide compounds [12].

The electrochemical methods also need to modify the electrodes to optimize the sensor properties. Currently, the nanostructure has been applied to modify the sensors due to high surface area and stability [13]. Among the nanostructures, metallic nanostructures with high stability and high electrical conductivity show the excellent sensing properties. For example, silver nanostructures enhance the electron transfer rate in electrochemical activities due to high electron density in conductance band [14]. Silver can be synthesized in various structures such as nano-wires, nano-particles, nano-leaves, core-shell nanoprisms and nano-dendrites [15-17]. Moreover, silver nanostructures can be used to detect organic, inorganic and biochemical analytes.

In this study, Ag NPs/CNTs/GC electrode was applied for the determination of cyanide as a contamination in food products. First, Ag NPs/CNTs were synthesized chemically and applied to modify the GC electrode surface. Then, the structural properties of synthesized Ag NPs/CNTs were studied by SEM, EDX and XRD analyses. Finally, electrochemical methods were used to investigate the response of the modified electrode to the cyanide sensing properties.

2. EXPERIMENTAL

Purchased CNTs were dissolved in a mixture of concentrated H_2SO_4 and HNO_3 (4:1, v/v), and refluxed for 240 minutes to synthesize carboxylated CNTs. Then, the centrifugation at 5000 rpm was applied to separate the obtained CNTs. Finally, CNTs was rinsed with double distilled water.

The functionalized CNTs (0.5 mM) in a flask were dispersed in an ultrasonic bath for 150 seconds at 50kHz. Then, 50 mM of AgNO_3 solution was injected in dispersed CNTs solution. After 24 hours, the Ag NPs/CNTs were synthesized without additional reducing reagent. Finally, Ag NPs/CNTs were collected by centrifuging process.

In order to prepare the CNTs/GC and Ag NPs/CNTs/GC electrodes, in the first step, the GC electrodes was cleaned as the following process: a) the GC surface was soft polished with 1, 0.3 and 0.05 μm of alumina for 20 minutes, b) the tip of GC electrodes was ultra-sonicated in ethanol and distilled water for 20 min, respectively. Then, 15 μL of an ethanol suspension containing 1.0 mg/mL of MWCNT or Ag NPs/CNTs was dropped on the cleaned GC surface and dried in the room temperature.

The morphology of synthesized CNTs was analyzed by scanning electron microscopy (FESEM, Philips FEI XL30 SFEG). Crystal structure of CNTs and Ag NPs/CNTs were investigated with Xpert Pro X-ray diffractometer with 1.5404 \AA (Cu $K\alpha$) in wavelength and 40KV/30 mA in power.

Electrochemical studies were performed on the three-electrode cells which contained Ag/AgCl/(sat KCL) and Pt wire as a reference and counter electrode, respectively. GC, CNTs/GC and Ag NPs/CNTs/GC electrodes were used as the working electrodes. Autolab modular electrochemical system (Eco. Chemieul Techt) was used for voltammetry and amperometry studies. The 0.1 M phosphate buffer solutions were provided from H_3PO_4 and NaH_2PO_4 . The pH of phosphate buffer solutions was applied with HCl and NaOH solution to adjust the pH. Cyanide sodium was used to prepare the cyanide solution.

In order to consider the real sample, fresh apricot were purchased from the market, peeled, washed with water, cut into smaller pieces and squeezed to obtain juices (2000E-6, Changzhou Xunke Commercial Equipment CO., LTD. China). The prepared apricot juice was passed through the filter. The obtained transparent and pure solution of apricot was added in 0.1 M phosphate buffer solutions (1:1, v/v) in pH 7.0.

3. RESULT AND DISCUSSION

Figure 1a and b show the FESEM images of synthesized CNTs and Ag/CNTs. The high aspect ratio of CNTs and Ag/CNTs is observed. As shown in figure 1a, the average diameter of CNTs are found at 85 nm. The average size of Ag nanoparticles attached to the CNTs are found to be 65 nm. As shown, the obtained high porosity and high aspect ratio for the samples lead to a high effective surface area of modified electrode which can promote the properties of the sensor to determine the analytes. Figure 1c shows the EDX responses of the samples averaged over several randomly chosen sample regions, indicating the peaks corresponding to silver and CNTs.

Figure 1d shows the XRD patterns of CNTs and Ag/CNTs. The diffraction peaks at 38.89°, 45.09°, 65.07°, and 77.98° corresponds to (111), (200), (220), and (311) the reflections of fcc phase of silver are in good agreement with the standard JCPDF data reference (No. 04-0783) [18]. The peaks indicate the face centered cubic (fcc) structure of the silver nanoparticles. The peak (002) at 25.87° is corresponding to carbon nanotubes oriented along the c-axis and it is in agreement with the standard JCPDF data reference (No. 58-1638). The broad peaks indicate the presence of nanostructured crystalline Ag nanoparticles.

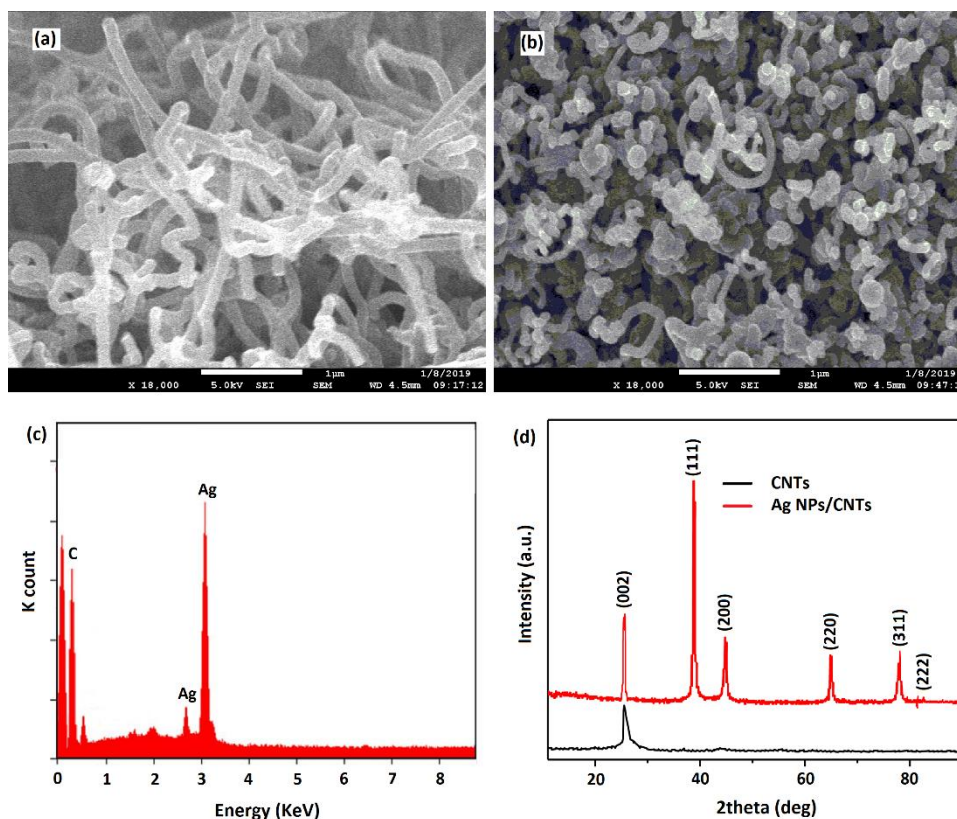


Figure 1. FESEM images of (a) CNTs and (b) Ag/CNTs, (c) EDX of Ag/CNTs sample, and (d) XRD pattern synthesized CNTs and Ag NPs/CNTs.

There is a clear positive synergistic effect when MWCNT and Ag NPs are combined as modifiers in the same electroanalytical platform. The electro-catalytic properties, sensitivity and magnitude can be dramatically enhanced when the nanotubes are decorated with other nanomaterials [19, 20]. These characteristics justify the different cyclic voltammograms shown in figure 2. As can be seen, MWCNT/GCE presents a larger currents in comparison to unmodified GCE, probably due to the expansion of the surface area provided by the functionalized nanostructures [21]. Such effect is also observed for Ag NPs /MWCNT/GCE, but in the latter case the performance is even higher, confirming the advantages obtained when the modifiers are used in association. Furthermore, these data also shows that the deposited Ag NPs on MWCNT films can potentiates the advantages observed for the isolated carbon nanomaterials.

All cyclic voltammetric studies of modified and unmodified electrodes were performed in 0.1 M phosphate buffer solution with pH 7.0 at a scan rate of 20 mV s^{-1} in the potential range of -0.50 to 1.0 V. Figure 2 column (I) shows the recorded cyclic voltammograms of GC, CNTs/GC and Ag NPs/CNTs/GC electrodes. As shown in figure 2, no oxidation or reduction peak is observed for the GC and CNTs/GC electrodes in absent of cyanide in the electrolyte. Figure 2(c) shows the well-defined redox peaks for Ag NPs/CNTs/GC electrode in -0.18 V and 0.28 V because of oxidation and reduction of Ag NPs in absent of cyanide in the electrolyte, respectively. When $50 \mu\text{M}$ of cyanide solution was injected in electrolyte, the recorded cyclic voltammograms show a sharp peak at 0.72V for GC, CNTs/GC and Ag NPs/CNTs/GC electrodes due to oxidation of cyanide [22]. Figure 2(c) shows addition

of cyanide lead to an increase in the reduction and oxidation peak of Ag NPs/CNTs/GC electrode. It can indicate the Ag NPs catalyzed reduction and oxidation of cyanide. There is more current for the observed oxidation peak in Ag NPs/CNTs/GC electrode that refers to the higher sensitivity response to cyanide determination. High current oxidation of silver can be related to its high conductivity due to its high electron concentration and high Fermi surface area [23].

In order to study the stability response of all electrode for oxidation behavior of cyanide, the successive cycle voltammograms of 50 μM of cyanide in 0.1 M phosphate buffer solution were recorded. Figure 2 column (II) shows after 100th recorded successive cycle voltammograms, the changes of cyanide oxidation current at 0.72 V for GC, CNTs/GC and Ag NPs/CNTs/GC are more than 67%, 36% and less than 6%, respectively. Therefore, Ag NPs/CNTs/GC electrode surface shows more stable and sensitive response to determine cyanide. As a result, Ag NPs/CNTs/GC electrode can be selected as a sensor for more electrochemical study of the cyanide determination.

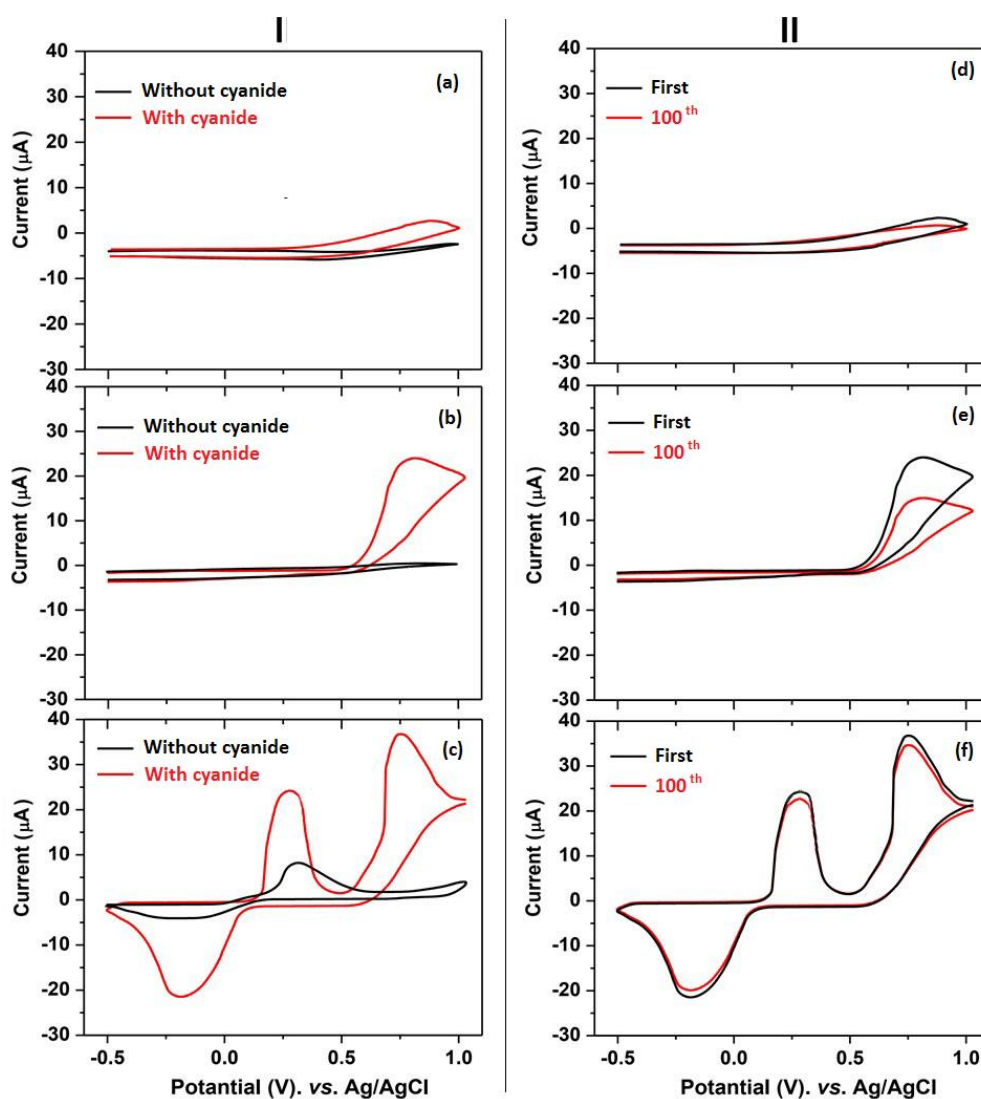


Figure 2. I: Recorded cyclic voltammograms in without and with 50 μM cyanide solution for (a) GC, (b) CNTs/GC and (c) Ag NPs/CNTs/GC electrodes. II: First and 100th Recorded cyclic voltammograms of (d) GC, (e) CNTs/GC and (f) Ag NPs/CNTs/GC electrodes after injection of 50 μM cyanide solution.

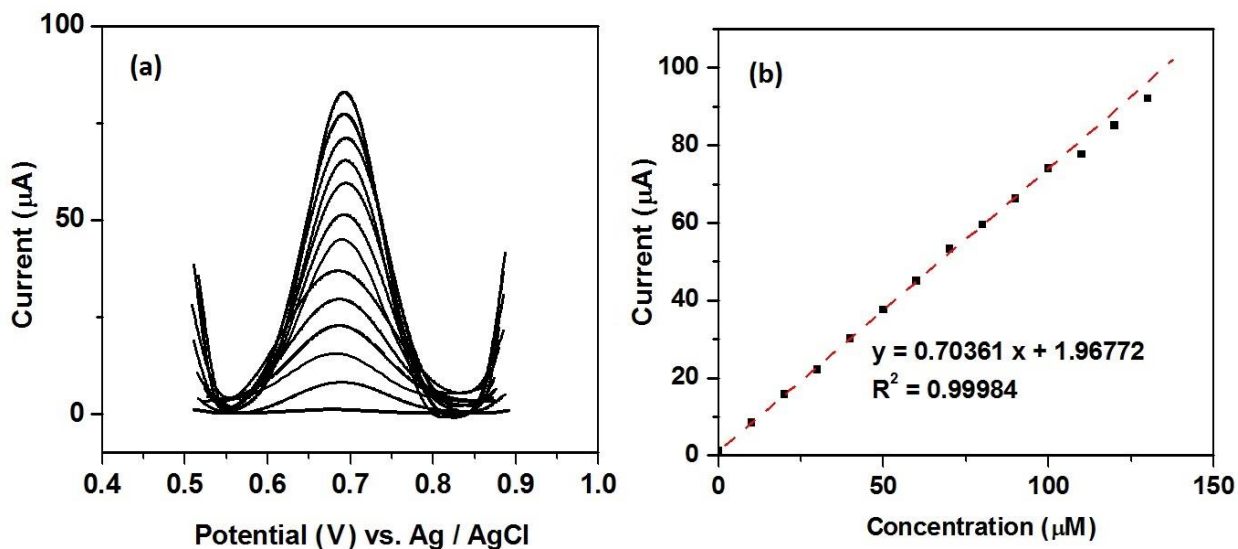


Figure 3. (a) The recorded square wave voltammograms of Ag NPs/CNTs/GC electrode in 0.1 M phosphate buffer solution in successive additions of 10 µM cyanide solution; (b) the plots of calibration graphs.

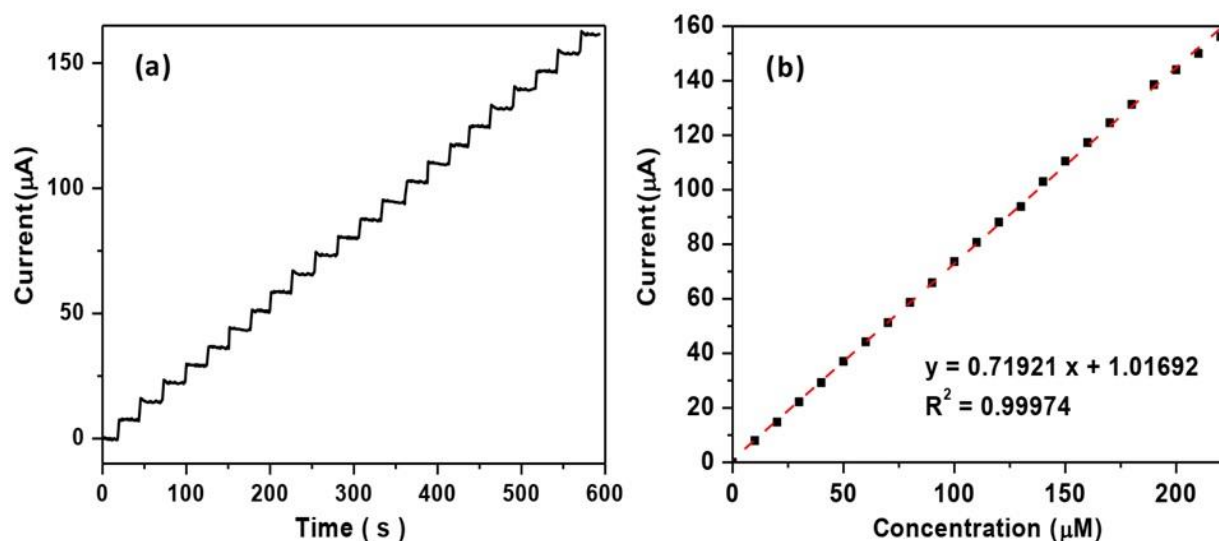


Figure 4. (a) The amperometric response of Ag NPs/CNTs/GC electrode in 0.1 M phosphate buffer solution in successive additions of 10 µM cyanide solution; (b) the plots of calibration graphs.

In order to evaluate the cyanide concentration effects, the square wave voltammetric studies of Ag NPs/CNTs/GC electrode was performed in 0.1 M phosphate buffer solution at pH value of 7.0. Figure 3a shows the recorded square wave voltammograms in successive injections of 10 µM cyanide solution. The calibration graphs in Figure 3b exhibits the equation current (µA) = 0.7036 [concentration of cyanide (µM)] (µA/ µM) + 1.96772 (µA). The high correlation coefficient has proven the low dispersion of the data and shows that the mathematical model credibly describes the variance of the results. Furthermore, the square wave voltammetry study showed the linear range, sensitivity and detection values are 0.1 to 100 µM, 0.7036 µA/ µM and 4 nM, respectively. The detection limit was similar to those obtained by highly accurate and selective methods involving chemiluminescence [24], capillary electrophoresis [25,

26], ion [27, 28] and liquid chromatography [29], but able to overcome issues in terms of quickness, analytical and instrumental costs, waste generation and operational simplicity.

Amperometry as an electrochemical technique is relatively precise method to investigate sensor characterizations such as linear range, detection limit, sensitivity, and selectivity [30]. Figure 4a shows the amperometric response of Ag NPs/CNTs/GC electrode in 0.1 M phosphate buffer solution pH 7.0 in successive injections of 10 μM cyanide solution. In all amperometric studies the electrode held at 0.7 V. Ag NPs/CNTs/GC electrode showed a well-defined step response. Increasing the Ag NPs loading in the multilayered assembly did not present any improvement in property and the linear range narrowed. The excellent electrochemical behavior for Ag NPs/CNTs/GC can be explained by the Ag NPs dispersion and surface properties. The porous structure derived from the amorphous nature of CNTs facilitated the dispersion of NPs into the matrix, which increased the specific area of these materials and improved catalytic efficiency [31, 32]. Also, due to the high electronic conductivity of the CNTs, charge was able to be transmitted along the chains towards the dispersed metals where the electrocatalytic reaction occurred [33]. Figure 4b indicates the calibration graphs as equation $\text{current } (\mu\text{A}) = 0.71921 [\text{concentration of cyanide } (\mu\text{M})] (\mu\text{A}/\mu\text{M}) + 1.01692 (\mu\text{A})$. Therefore, the amperometry study revealed the linear range, sensitivity and detection values were 0.1 to 210 μM , 0.7192 $\mu\text{A}/\mu\text{M}$ and 4 nM, respectively.

Table 1. Comparison of Ag NPs/CNTs/GC sensor performance with other cyanide sensors.

Electrodes	Technique	detection limit (μM)	Linear range (μM)	Sensitivity ($\mu\text{A}/\mu\text{M}$)	Ref.
glassy carbon electrode modified with graphene oxide and titanium dioxide nanoparticles	Amperometry	0.1	0.1–60	165.5	[35]
horseradish peroxidase immobilization on gold sononanoparticles	Amperometry	0.03	0.1–58.6	3.5	[36]
gold nanoparticles decorated carbon ceramic	Square wave voltammetry	0.09	0.5-1.4	2.41	[37]
silver sulfide nanoparticles and hierarchical porous carbon modified carbon paste	Square wave voltammetry	0.07	0.59–1100	1.1	[34]
polyethylene glycol coated cadmium sulfide nanoparticles	Cycle voltammetry	0.09	0.009-4.2	42.5	[38]
Ag NPs/CNTs/glassy carbon	Amperometry	0.004	0.1-210	0.7192	This work
Ag NPs/CNTs/glassy carbon	Square wave voltammetry	0.004	0.1-100	0.7036	This work

Table 1 shows a comparative study on the main parameters obtained in this research and the other cyanide electrochemical sensors. The results of amperometric and square wave voltammetric techniques illustrated that the calculated sensitivity and linear wide range in amperometric technique had larger values than the square wave voltammetric technique. In amperometric technique, electrode was stirred

(rotation speed 1000 rpm) and fresh solution reached the electrode surface in every time. Hence, sensitivity and linear range in this technique are bigger than square wave voltammetric technique. Moreover, the results illustrate that the electrochemical method has a low detection limit which are better than the other reported cyanide electrochemical sensors. It can be deduced that the Ag NPs/CNTs/GC electrode can be applied for a study of a low concentration cyanide such as in fruits. The wide linear range is seen for silver sulfide nanoparticles and hierarchical porous carbon modified carbon paste (0.59 – 1100 μM) [34] and Ag NPs/CNTs/GC (0.1-100 μM) electrodes through the square wave voltammetric technique. It can be concluded that the silver nanoparticles compositions have high porosity and more sensitive site on electrode surface. Thus, the site saturation occurred in high concentration ($> 1100 \mu\text{M}$ for modified electrode in [34] and $> 100 \mu\text{M}$ for this study) in comparison with the other cyanide sensors.

Figure 5a shows the amperometric response of 50 μM cyanide solution during a prolonged 10 minutes. As seen, the response $\sim 9\%$ decreases in current 10 minutes after injection. Thus, the amperometric response of Ag NPs/CNTs/GC electrode in paracetamol is stable.

In order to study the selectivity response of Ag NPs/CNTs/GC electrode as nitrite sensor, the amperometric studies was performed in the presence of different analytes [39]. Figure 5b reveals the recorded amperogram of Ag NPs/CNTs/GC electrode in 0.1 M phosphate buffer solution pH 7.0. As shown, two successive additions of 10 μM cyanide solution followed by successive additions of 50 μM of Br^- , SO_3^{2-} , CH_3COO^- , I^- , $\text{C}_2\text{O}_4^{2-}$ and Cl^- analytes, and then two successive additions of 10 μM cyanide solution. Then, successive additions of 50 μM of SO_4^{2-} , CO_3^{2-} , Ni^{+2} , Co^{2+} , HPO_4^{-2} , F^- and Zn^{+2} solutions were performed. Finally, three successive additions of 10 μM cyanide were done. The results indicated that the modified electrode showed a clear response to all additions of cyanide solution. However, the modified electrode did not show any significant response for the other analytes. Furthermore, the modified Ag NPs/CNTs/GC electrode indicated a selective response to cyanide in the presence of the above analytes. Therefore, the above analytes do not interfere in the determination of cyanide on Ag NPs/CNTs/GC electrode surface which exhibited an excellent selectivity for cyanide.

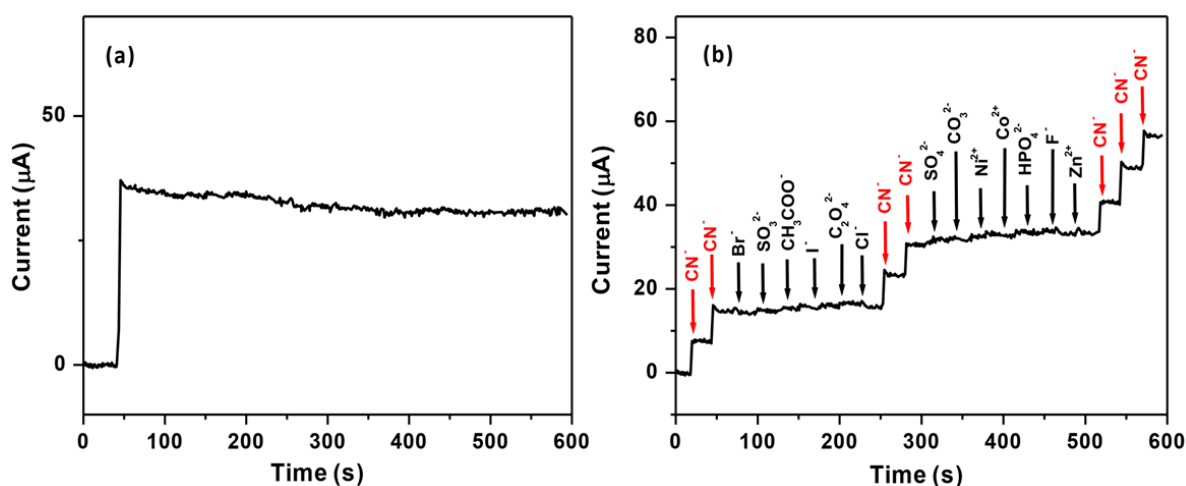


Figure 5. The amperometric response of Ag NPs/CNTs/GC electrode in 0.1 M phosphate buffer solution (a) for 50 μM addition of cyanide during 10 minutes and (b) for 10 μM addition of cyanide and 50 μM addition of Br^- , SO_3^{2-} , CH_3COO^- , I^- , $\text{C}_2\text{O}_4^{2-}$, Cl^- , SO_4^{2-} , CO_3^{2-} , Ni^{+2} , Co^{2+} , HPO_4^{-2} , F^- and Zn^{+2} solutions.

In order to study the Ag NPs/CNTs/GC electrode for the determination of cyanide in real samples, the concentration of cyanide was measured in prepared sample of apricot juice [40]. The standard injection of cyanide was applied to determine the cyanide in the sample. Figure 6a shows the amperometric response of Ag NPs/CNTs/GC electrode for apricot juice in successive injections of 0.01 mM cyanide solution. Figure 6b reveals the calibration curve as current (μA) = 736.2921[concentration of cyanide (mM)] ($\mu\text{A}/\text{mM}$) + 8.01107 (μA) with a correlation coefficient of 0.99674. The intercept point of the calibration curve equation with the concentration axis, the concentration of cyanide in the real sample of electrochemical cell and pure apricot juice were estimated as 0.001mM and 0.0005 mM, respectively.

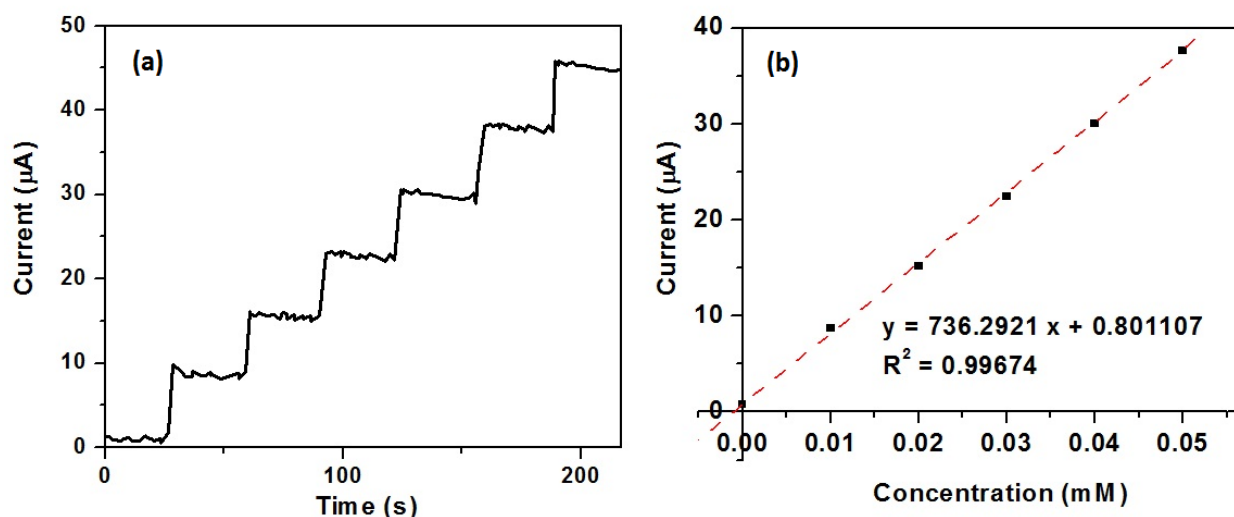


Figure 6. (a) The amperometric response of Ag NPs/CNTs/GC electrode in 0.1 M phosphate buffer solution in 0.01 mM cyanide concentration in apricot juice at a scan rate of 20 mV s^{-1} ; (b) Plot of calibration curve.

4. CONCLUSION

In this study, the Ag NPs/CNTs/GC electrode was successfully used for electrochemical determination of cyanide as contaminant in water and fruits. Ag NPs/CNTs nanostructures were synthesized through chemical approach for modification of the glassy carbon surface. The structural properties of synthesized CNTs and Ag NPs/CNTs were studied by SEM, EDX and XRD analyses. The structural studies showed high density, porosity and aspect ratio of the modified electrodes. The cycle voltammetric studies of Ag NPs/CNTs/GC electrode showed a sharp and stable oxidation peak at 0.75 V in pH 7 for cyanide. High sensitive, selective and stable for the determination of cyanide was observed in amperometry results of Ag NPs/CNTs/GC electrode. The linear range, sensitivity, and detection limit of cyanide modified sensor were 0.1 to 210 μM , 0.7192 $\mu\text{A}/\mu\text{M}$ and 4 nM, respectively. The amperometric response results of real sample showed the modified electrode was successfully applied to cyanide detection in apricot juice. The study on the interfere effect of Br^- , SO_3^{2-} , CH_3COO^- , I^- , $\text{C}_2\text{O}_4^{2-}$, Cl^- , SO_4^{2-} , CO_3^{2-} , Ni^{+2} , Co^{2+} , HPO_4^{-2} , F^- and Zn^{+2} analytes showed that there was no interfere in the

determination of cyanide on Ag NPs/CNTs/GC electrode surface. Low detection limit, high sensitivity and high stability of the modified sensor for cyanide detection introduced Ag NPs/CNTs/GC electrode as an alternative electrochemical sensor which can be used to detect toxic substances in food products.

ACKNOWLEDGEMENT

This work was sponsored in part by National Natural Science Foundation of China (21573003), Ph.D. Research launch Fund of Baicheng Normal University (BSQD20170417).

References

1. J. Spink, D.L. Ortega, C. Chen and F. Wu, *Trends in Food Science & Technology*, 62 (2017) 215.
2. H. Chen, S. Zhang, Z. Zhao, M. Liu and Q. Zhang, *Progress in Chemistry*, 31 (2019) 571.
3. D. Yuan, C. Zhang, S. Tang, X. Li, J. Tang, Y. Rao, Z. Wang and Q. Zhang, *Water research*, 163 (2019) 114861.
4. J. Rouhi, S. Mahmud, S.D. Hutagalung and S. Kakooei, *Journal of Micro/Nanolithography, MEMS, and MOEMS*, 10 (2011) 043002.
5. M. Untang, J. Shiowatana and A. Siripinyanond, *Analytical Methods*, 2 (2010) 1698.
6. T.A. Ali, G.G. Mohamed, A.L. Saber and L.S. Almazroai, *International Journal of Electrochemical Science*, 12 (2017) 11904.
7. K. Akben and S. Timur, *International Journal of Electrochemical Science*, 13 (2018) 3855.
8. F. Husairi, J. Rouhi, K. Eswar, A. Zainurul, M. Rusop and S. Abdullah, *Applied Physics A*, 116 (2014) 2119.
9. D. Udhayakumari, *Sensors and Actuators B: Chemical*, 259 (2018) 1022.
10. J. Ma and P.K. Dasgupta, *Analytica chimica acta*, 673 (2010) 117.
11. S. Tang, N. Li, D. Yuan, J. Tang, X. Li, C. Zhang and Y. Rao, *Chemosphere*, 234 (2019) 658.
12. P. Shao, J. Tian, F. Yang, X. Duan, S. Gao, W. Shi, X. Luo, F. Cui, S. Luo and S. Wang, *Advanced Functional Materials*, 28 (2018) 1705295.
13. H. Savaloni, R. Savari and S. Abbasi, *Current Applied Physics*, 18 (2018) 869.
14. X. He, F. Deng, T. Shen, L. Yang, D. Chen, J. Luo, X. Luo, X. Min and F. Wang, *Journal of colloid and interface science*, 539 (2019) 223.
15. B. Hu, J. Huang and L. Wang, *ChemistrySelect*, 3 (2018) 8514.
16. S. Mohan, F. Okumu, O. Oluwafemi, M. Matoetoe and O. Arotiba, *International Journal of Electrochemical Science*, 11 (2016) 745.
17. P. Shao, J. Tian, X. Duan, Y. Yang, W. Shi, X. Luo, F. Cui, S. Luo and S. Wang, *Chemical Engineering Journal*, 359 (2019) 79.
18. B. Khoshnevisan, M. Behpour, S. Ghoreishi and M. Hemmati, *International journal of hydrogen energy*, 32 (2007) 3860.
19. L.A. Goulart, R. Gonçalves, A.A. Correa, E.C. Pereira and L.H. Mascaro, *Microchimica Acta*, 185 (2018) 12.
20. W.D.A. Paiva, T.M.B. Oliveira, C.P. Sousa, P. de Lima Neto, A.N. Correia, S. Morais, D.R. Silva and S.S.L. Castro, *Journal of The Electrochemical Society*, 165 (2018) B431.
21. P. Shao, L. Ding, J. Luo, Y. Luo, D. You, Q. Zhang and X. Luo, *ACS applied materials & interfaces*, 11 (2019) 29736.
22. R. Berenguer, C. Quijada, A. La Rosa-Toro and E. Morallón, *Separation and Purification Technology*, 208 (2019) 42.
23. P. Shao, X. Duan, J. Xu, J. Tian, W. Shi, S. Gao, M. Xu, F. Cui and S. Wang, *Journal of hazardous materials*, 322 (2017) 532.
24. M. Amjadi, J. Hassanzadeh and J.L. Manzoori, *Microchimica Acta*, 181 (2014) 1851.

25. Q. Zhang, N. Maddukuri and M. Gong, *Journal of Chromatography A*, 1414 (2015) 158.
26. L. Yang, G. Yi, Y. Hou, H. Cheng, X. Luo, S.G. Pavlostathis, S. Luo and A. Wang, *Biosensors and Bioelectronics*, 141 (2019) 111444.
27. O. Destanoğlu, G. Gümüş Yılmaz and R. Apak, *Journal of Liquid Chromatography & Related Technologies*, 38 (2015) 1537.
28. E. Jaszczak, M. Ruman, S. Narkowicz, J. Namieśnik and Ż. Polkowska, *Journal of analytical methods in chemistry*, 2017 (2017) 1.
29. R.K. Bhandari, E. Manandhar, R.P. Oda, G.A. Rockwood and B.A. Logue, *Analytical and bioanalytical chemistry*, 406 (2014) 727.
30. J. Rouhi, S. Mahmud, S.D. Hutagalung and N. Naderi, *Electronics letters*, 48 (2012) 712.
31. D. Zhai, B. Liu, Y. Shi, L. Pan, Y. Wang, W. Li, R. Zhang and G. Yu, *ACS nano*, 7 (2013) 3540.
32. R.-C. Zhang, D. Sun, R. Zhang, W.-F. Lin, M. Macias-Montero, J. Patel, S. Askari, C. McDonald, D. Mariotti and P. Maguire, *Scientific reports*, 7 (2017) 46682.
33. A. Malinauskas, *Synthetic Metals*, 107 (1999) 75.
34. A.A.C. Riojas, A. Wong, G.A. Planes, M.D. Sotomayor, A. La Rosa-Toro and A.M. Baena-Moncada, *Sensors and Actuators B: Chemical*, 287 (2019) 544.
35. R. Hallaj and N. Haghghi, *Microchimica Acta*, 184 (2017) 3581.
36. A. Attar, L. Cubillana-Aguilera, I. Naranjo-Rodríguez, J.L.H.-H. de Cisneros, J.M. Palacios-Santander and A. Amine, *Bioelectrochemistry*, 101 (2015) 84.
37. M. Shamsipur, Z. Karimi and M.A. Tabrizi, *Microchemical Journal*, 133 (2017) 485.
38. K. Salariya, A. Umar, S.K. Kansal and S.K. Mehta, *Sensors and Actuators B: Chemical*, 241 (2017)
39. N. Naderi, M. Hashim and J. Rouhi, *International Journal of Electrochemical Science*, 7 (2012) 8481.
40. J. Rouhi, S. Mahmud, S. Hutagalung and S. Kakooei, *Micro & Nano Letters*, 7 (2012) 325.